Acta Cryst B
STRUCTURAL SCIENCE
CRYSTAL ENGINEERING
MATERIALS
ISSN 2052-5206

Halogen bonding stabilizes a *cis*-azobenzene derivative in the solid state: a crystallographic study

Marco Saccone,[a] Antti Siiskonen,[a] Franisco Fernandez-Palacio,[b] Arri Priimagi,[a]* Giancarlo Terraneo,[b]* Giuseppe Resnati[b] and Pierangelo Metrangolo[b,c]

[a]Laboratory of Chemistry and Bioengineering, Tampere University of Technology, PO Box 541, FI-33101 Tampere, Finland, [b]Laboratory of Nanostructured Fluorinated Materials (NFMLab), Department of Chemistry, Materials and Chemical Engineering 'Giulio Natta', Politecnico di Milano, Via L. Mancinelli 7, 20131 Milano, Italy, and [c]HYBER Centre of Excellence, Department of Applied Physics, Aalto University, PO Box 15100, FI-02150 Espoo, Finland. *Correspondence e-mail: arri.priimagi@tut.fi, giancarlo.terraneo@polimi.it

Received 1 January 2017
Accepted 2 March 2017

Edited by A. J. Blake, University of Nottingham, England

Keywords: azobenzene; halogen bonding; isomerization.

CCDC references: 1449803; 1449806

Supporting information: this article has supporting information at journals.iucr.org/b

Crystals of *trans*- and *cis*-isomers of a fluorinated azobenzene derivative have been prepared and characterized by single-crystal X-ray diffraction. The presence of F atoms on the aromatic core of the azobenzene increases the lifetime of the metastable *cis*-isomer, allowing single crystals of the *cis*-azobenzene to be grown. Structural analysis on the *cis*-azobenzene, complemented with density functional theory calculations, highlights the active role of the halogen-bond contact (N···I synthon) in promoting the stabilization of the *cis*-isomer. The presence of a long aliphatic chain on the azobenzene unit induces a phase segregation that stabilizes the molecular arrangement for both the *trans*- and *cis*-isomers. Due to the rarity of *cis*-azobenzene crystal structures in the literature, our paper makes a step towards understanding the role of non-covalent interactions in driving the packing of metastable azobenzene isomers. This is expected to be important in the future rational design of solid-state, photoresponsive materials based on halogen bonding.

1. Introduction

Azobenzenes are molecules containing two aromatic rings held together by a nitrogen–nitrogen double bond. Due to the N=N link, they exist in two stereoisomeric forms, *trans* and *cis*, and it is possible to switch the former to the latter and *vice versa* by absorption of UV–vis photons (Zhao & Ikeda, 2009; Dhammika Bandara & Burdette, 2012). The *trans*-form is usually more thermodynamically stable than the *cis*-form, which is kinetically not persistent in ambient conditions (Hoffmann, 1987; Hoffmann *et al.*, 2008). Recently there has been considerable interest towards long-lived *cis*-azobenzenes from the perspective of making bistable systems that can be reversibly switched with light (Bléger & Hecht, 2015; Beharry *et al.*, 2011; Weston *et al.*, 2014). For example, Woolley and collaborators, based on previous work by Herges *et al.* (Siewertsen *et al.*, 2009), reported on the exceptional photoswitching behavior of the 5,6-dihydrodibenzo[*c*,*g*][1,2]diazocine (Fig. 1*a*) that has been used to exert a reversible and efficient photocontrol over the conformation of a peptide (Samanta *et al.*, 2012). In their case the *cis*-form is the more thermodynamically stable isomer. More recently Bléger and coworkers showed that the *cis*-forms of some *ortho*-fluorinated azobenzenes (Fig. 1*b*) possess an impressive kinetic stability in solution, with *cis–trans* thermal lifetimes up to several months or even a year (Bléger *et al.*, 2012; Knie *et al.*, 2014).

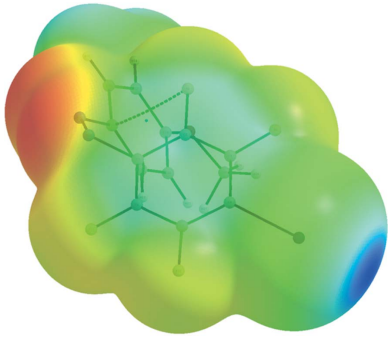

Bushuyev *et al.* have used the aforementioned *ortho*-fluorinated azobenzenes to produce mechanical motion upon irradiation of an azobenzene crystal. The mechanical motion has been attributed to the isomerization of azobenzenes in the crystalline state (Bushuyev, Corkery *et al.*, 2014; Bushuyev, Tomberg *et al.*, 2014). Our interest in fluorinated azobenzenes started in 2012 when we developed halogen-bonded photoresponsive polymeric and liquid-crystalline materials, demonstrating that halogen bonding is an efficient supramolecular tool for light-induced surface patterning and photoalignment (Priimagi, Cavallo *et al.*, 2012; Priimagi, Saccone *et al.*, 2012; Saccone *et al.*, 2015). Subsequently, we developed a small library of halogen-bonded liquid crystals based on fluorinated azobenzenes that undergo a rich variety of photoinduced phase transitions upon light irradiation (Fernandez-Palacio, Poutanen *et al.*, 2016). These results were achieved thanks to the unique characteristics of halogen bonding, namely its strength and directionality (Saccone *et al.*, 2013) that allow this interaction to influence the solid-state structure even in the presence of stronger competing interactions (Corradi *et al.*, 2000). Given the fact that many intriguing applications, *e.g.* fabrication of bistable light-activated devices and actuators (Iamsaard *et al.*, 2016), depend on properties of the azobenzene molecules in the solid state, it is perhaps surprising that the solid-state structural analysis of *cis*-azobenzenes is rather unexplored. A recent search revealed that only 30 crystal structures having the azo moiety in the *cis*-form are reported in the Cambridge Structural Database (CSD; Groom *et al.*, 2016; Bushuyev *et al.*, 2015). This finding confirms the significant difficulty in crystallizing *cis*-azobenzenes and highlights the lack of structural information related to these metastable systems. However, although few, these 30 crystal structures possess some common structural features that can be used as design guidelines for obtaining stable *cis*-azobenzene crystals. Specifically, half of the reported *cis*-crystals contain aromatic units that are fully or partially fluorinated, indicating the importance of fluorination in providing a kinetically persistent *cis*-form (Bléger *et al.*, 2012; Knie *et al.*, 2014). Another important structural feature is that all the fluorinated *cis*-azobenzenes are highly symmetrical and 'simple', both aromatic rings being decorated with the same functionalities (*e.g.* F, Br or I atoms), while not having long pendants such as alkyl/alkoxy chains.

Obtaining crystals of *cis*-azobenzenes is pertinent in the field of photoresponsive materials design, that becomes evermore challenging when targeting non-symmetric *cis*-azobenzenes with aliphatic pendants. To achieve this goal, and to understand what non-covalent interactions contribute to stabilizing non-symmetric azobenzenes in the solid state, we focus our attention on the *trans*- and *cis*-forms of the fluorinated azobenzene shown in Fig. 2, labeled here **TRANS**$_{azo}$ and **CIS**$_{azo}$. Knowing that fluorination of the ring close to the azo group increases the lifetime of the *cis*-form, our aim was (i) to evaluate whether the presence of a halogen-bond donor site on the azobenzene unit (the I atom) contributes to stabilizing the *cis*-isomer in the solid state, and (ii) to study the role of long alkyl chains on the crystal packing of *cis*-azobenzenes. The obtained results highlight the importance of halogen bonding in the stabilization of the *cis*-crystal while in the *trans*-crystal, no halogen bond is detected. The aliphatic chain, in turn, acts as a stabilizing structural motif in both *trans*- and *cis*-crystals, inducing phase segregation from the aromatic core. Our structural analysis is complemented by theoretical calculations that shed further light on the role of halogen bonding and the fluorinated residue in stabilization of the *cis*-isomer.

2. Experimental

2.1. Materials

The **TRANS**$_{azo}$ molecule was synthesized as previously reported (Fernandez-Palacio, Poutanen *et al.*, 2016). Its photoisomerization properties have been studied in dilute dimethylformamide solution upon irradiation with UV light (365 nm), and the lifetime of the *cis*-isomer was found to be *ca* 12 days (Fernandez-Palacio, Poutanen *et al.*, 2016). The long *cis*-lifetime enabled us to obtain crystals of **CIS**$_{azo}$, upon illumination at 395 nm wavelength of a concentrated solution of **TRANS**$_{azo}$ and subsequent solvent evaporation. Single crys-

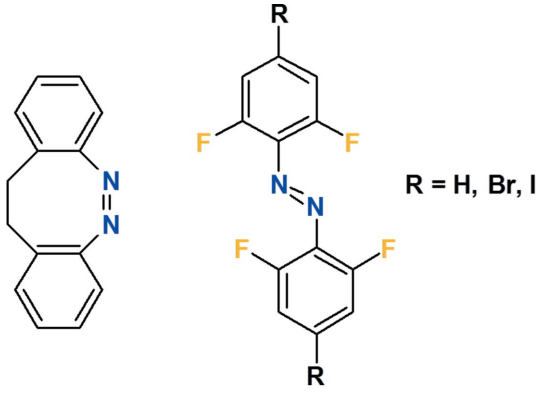

Figure 1
Examples of molecules having a kinetically persistent *cis*-isomer.

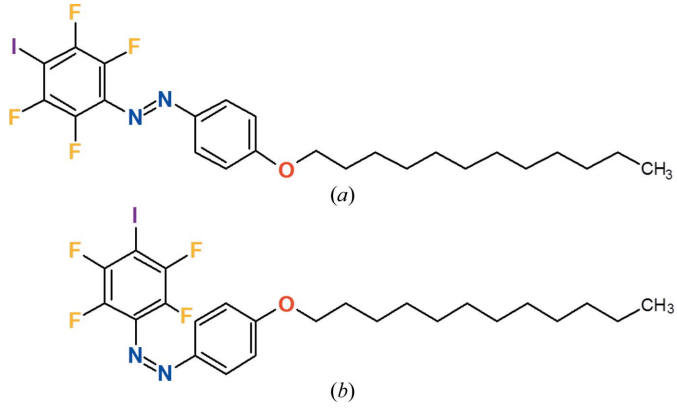

Figure 2
(*a*) The **TRANS**$_{azo}$ and (*b*) the **CIS**$_{azo}$ isomers of the azobenzene studied in the present work.

Table 1
Experimental details.

For both structures: $C_{24}H_{29}F_4IN_2O$, M_r = 564.39. Experiments were carried out at 103 K with Mo $K\alpha$ radiation using a Bruker APEXII CCD diffractometer. Absorption was corrected for by multi-scan methods (*SADABS*; Bruker, 2008). Refinement was on 290 parameters. H-atom parameters were not refined.

	TRANS$_{azo}$	**CIS**$_{azo}$
Crystal data		
Crystal system, space group	Triclinic, $P\bar{1}$	Monoclinic, $P2_1/c$
a, b, c (Å)	7.4374 (9), 10.2935 (12), 16.536 (2)	8.5802 (16), 33.663 (5), 8.752 (2)
α, β, γ (°)	105.237 (10), 101.641 (10), 95.607 (12)	90, 109.255 (16), 90
V (Å^3)	1181.0 (2)	2386.5 (8)
Z	2	4
μ (mm^{-1})	1.41	1.39
Crystal size (mm)	0.40 × 0.25 × 0.05	0.20 × 0.10 × 0.05
Data collection		
T_{min}, T_{max}	0.553, 0.706	0.791, 0.862
No. of measured, independent and observed [$I > 2\sigma(I)$] reflections	39 236, 10 045, 8800	25 224, 5073, 3840
R_{int}	0.028	0.047
(sin $\theta/\lambda)_{max}$ (Å^{-1})	0.822	0.650
Refinement		
R [$F^2 > 2\sigma(F^2)$], $wR(F^2)$, S	0.030, 0080, 1.07	0.037, 0.059, 1.05
No. of reflections	10 045	5073
$\Delta\rho_{max}$, $\Delta\rho_{min}$ (e Å^{-3})	1.39, −1.72	0.57, −0.99

Computer programs: *APEX*2, *SAINT*, *SADABS* (Bruker, 2008), *SIR*2002 (Burla *et al.*, 2003), *SHELXL*97 (Sheldrick, 2008), *Mercury* (Macrae *et al.*, 2008).

tals suitable for X-ray diffraction studies were obtained for both isomers by slow evaporation from chloroform solutions. The evaporation took place in the dark in order to prevent unwanted isomerization caused by ambient light, especially pertinent for obtaining the **CIS**$_{azo}$ crystals.

2.2. Computational details

Geometry minimization and complexation energy calculations were performed with *GAUSSIAN*09, Revision D.01 (Frisch *et al.*, 2009). The quantum theory of atoms in molecules (QTAIM) and interacting quantum atoms (IQA) analyses were performed with *AIMAll*, Version 16.10.31 (Keith, 2016). The geometries were optimized on a potential energy surface corrected for the basis-set superposition error (BSSE) using the counterpoise method implemented in *GAUSSIAN*09 (Boys & Bernardi, 1970). A frequency calculation was performed after the geometry minimization in order to confirm that the obtained geometry is a true minimum (*i.e.* no imaginary frequencies). The M06-2X/DGDZVP method was used for geometry optimization and to calculate the complexation energy (Siiskonen & Priimagi, 2017). To speed up the calculation, the long alkyl chain was truncated to methyl. The M06-2X/def2-TZVP method and the atom coordinates from the crystal structure were used to obtain the wavefunction for the QTAIM analysis.

2.3. Structure determination

The crystal data, data collection and structure refinement details are summarized in Table 1. The crystals were mounted in inert oil on glass fibers. Data were collected on a Bruker Kappa APEXII CCD diffractometer with Mo $K\alpha$ radiation (λ = 0.7107 Å) and a Bruker Kryoflex low-temperature device.

3. Results and discussion

3.1. Structural analysis of TRANS$_{azo}$

The molecule **TRANS**$_{azo}$ has been originally conceived with the purpose of obtaining a promesogenic molecule which, thanks to the halogen bond (Cavallo *et al.*, 2016), would produce supramolecular halogen-bonded liquid crystals featuring photoinduced phase transitions (Fernandez-Palacio, Poutanen *et al.*, 2016). Its structural design combines halogen-

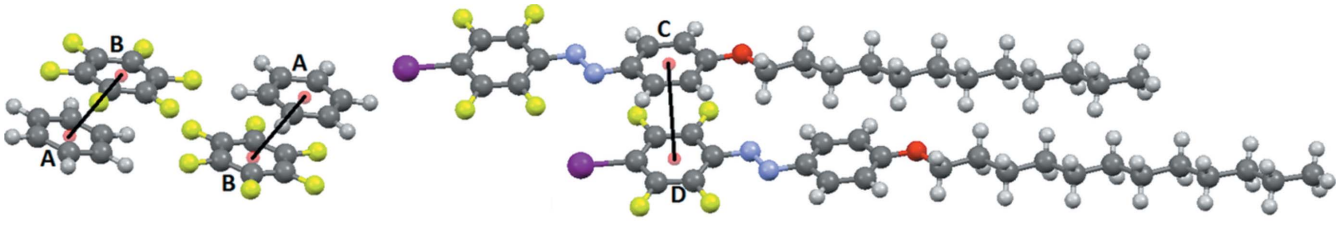

(*a*) (*b*)

Figure 3
Arene–perfluoroarene quadrupolar interactions as observed in BICVUE01 (*a*) and **TRANS**$_{azo}$ (*b*). The red dots denote the centroids of the aromatic rings.

bond-donating capability, a long lifetime of the *cis*-isomer, and a long aliphatic chain which typically promotes the appearance of liquid-crystal phases. The molecule crystallizes in the $P\bar{1}$ space group with the azo group exclusively adopting the *trans*-configuration (Fig. 3*b*). The two benzene rings are not coplanar and the angle between them is 9.71 (6)°.

The crystal packing is mainly driven by two kinds of intermolecular interactions. One of them is the arene–perfluoroarene quadrupolar interaction that occurs between molecules in neighboring planes. The observed distance between the centroids of the fluorinated and non-fluorinated rings is 3.72 (1) Å, very close to that of the benzene–hexafluorobenzene dimer (Fig. 3*a*; Williams *et al.*, 1992). This interaction may be strong, 25.54 kJ mol^{-1} for the benzene–hexafluorobenzene adduct (Řezáč *et al.*, 2012), and is very useful in crystal engineering (Salonen *et al.*, 2011), as well as in liquid-crystal self-assembly (Kishikawa, 2012). It is interesting to observe that the similarities in the crystals packing of the **TRANS**$_{azo}$ and the benzene–hexafluorobenzene dimer BICVUE01 also extend to the arrangement of the aromatic rings in neighboring planes as depicted in Fig. 4.

Secondly, the molecular arrangement is promoted by the H9···F1($-x, -y, -z$) hydrogen bond having the following geometrical parameters: C···F distance of 3.1477 (17) Å; C—H···F angle of 118.03 (8)°, which appear to be very similar in both structures (Fig. 4). In addition, the iodofluorinated ring further interacts with other neighboring molecules. Specifically, two F atoms show weak hydrogen-bond contacts with H atoms located at the terminal part of the aliphatic chains and the I atom points toward the methyl unit on the translated molecules ($-4 + x, y, -1 + z$). Finally, the crystal packing is stabilized by several C—H$_{(aliph)}$···C—H$_{(aliph)}$ interactions that induce the segregation of neighboring aliphatic chains from the azobenzene cores (Fig. 5). We have recently observed a similar segregation of aliphatic moieties from aromatic cores in a co-crystal structure where the **TRANS**$_{azo}$ molecule is combined with a 4,4′-alkoxystilbazole derivative (Fernandez-Palacio, Poutanen *et al.*, 2016), shown to be important when developing materials possessing liquid-crystalline properties (Tschierske, 2012). In the present structure, the I atom is not involved in any particular intermolecular interaction, and even the electron-rich N atoms of the azo-group are non-interacting, as derived by metric analysis. In contrast, the **CIS**$_{azo}$ structure is profoundly influenced by iodine–nitrogen interactions, as described below.

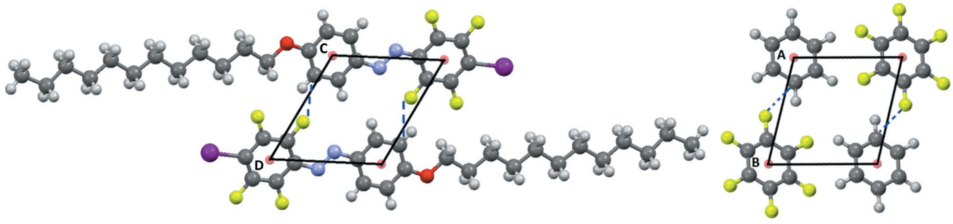

Figure 4
The arrangement of the aromatic rings is similar in **TRANS**$_{azo}$ (*a*) and in BICVUE01 (*b*). The red dots denote the centroids of the aromatic rings. The CD distance is 6.82 (1) Å and the AB distance is 6.85 (2) Å. The view is along the *c* axis. H···F hydrogen bonds are denoted with dotted blue lines.

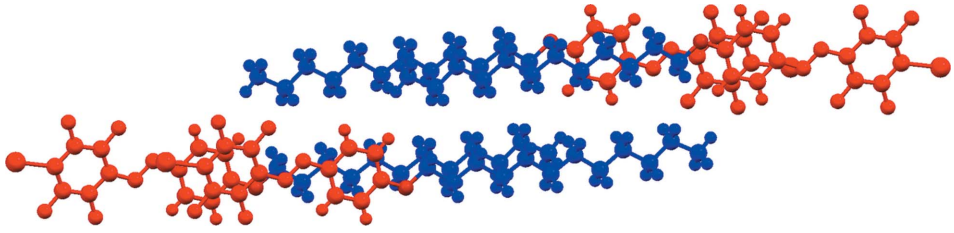

Figure 5
A view along the *c* axis of the overall packing of **TRANS**$_{azo}$ molecules, showing the segregation of the aliphatic regions (depicted in blue) from the aromatic cores (depicted in red).

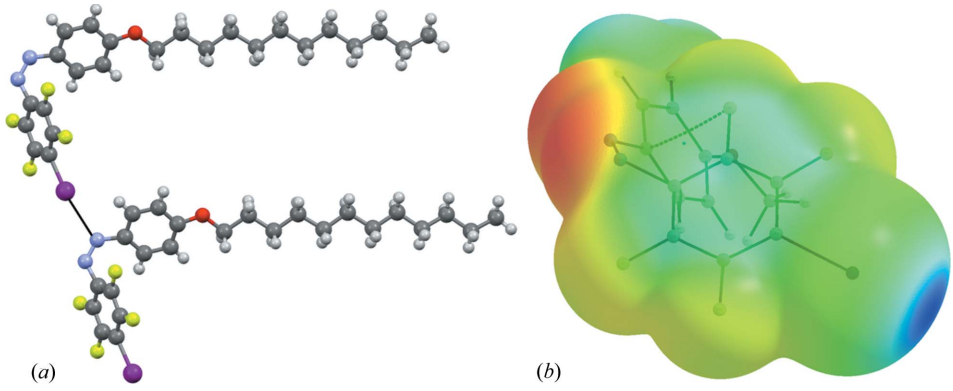

Figure 6
(*a*) The N···I halogen bond between the I atom and an N atom in the azo group; (*b*) the electrostatic potential of CIS$_{azo}$ computed at 0.001 a.u. of the electron density contour. Negative potential areas colored in red–yellow, positive potential areas colored in blue–cyan.

3.2. Structural analysis of CIS$_{azo}$

The **CIS**$_{azo}$ molecule is a metastable isomer of the **TRANS**$_{azo}$ molecule and its lifetime (*ca* 12 days in DMF solution), increased by fluorination, was long enough to allow us to prepare the *cis* single crystals and study their structural properties by X-ray diffraction analysis. Recently, the structures of some fluorinated *cis*-

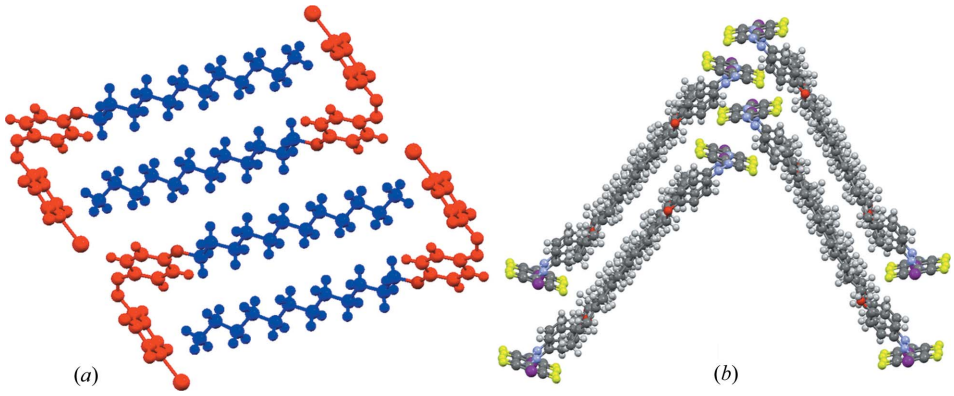

Figure 7
(*a*) Two-dimensional (along the *b* axis), and (*b*) three-dimensional view of the crystals packing of **CIS**$_{azo}$. The segregation of the aliphatic chains (blue) from the aromatic regions (red) is evident from (*a*), furthermore, the perfluorinated rings do not closely interact with the non-fluorinated rings as depicted in (*b*).

Table 2
IQA and QTAIM analysis.

Interaction	ρ(BCP)	$\nabla^2\rho$(BCP)	E_{inter}	E_{cl}	E_x
C···F	0.0108	0.0470	−24.10	−19.89	−4.21
C···H	0.0133	0.0472	−5.08	−1.76	−3.32

azobenzenes have been reported (Bushuyev, Corkery *et al.*, 2014; Bushuyev, Tomberg *et al.*, 2014), however, these papers concentrate solely on symmetrically substituted azobenzenes that lack long alkyl chains. This usually simplifies the crystallization process, but does not allow to infer the role of interactions that do not involve the aromatic moieties in the crystal packing. We address this issue in our analysis. The **CIS**$_{azo}$ form crystallizes in the $P2_1/c$ space group with the azo group quantitatively adopting the *cis*-form. The overall packing of the **CIS**$_{azo}$ molecule features several differences compared with the **TRANS**$_{azo}$. The most significant difference seems to be the presence of halogen bonding between the I atom in the tetrafluorophenyl ring and one of the N atoms of the azo moiety of another molecule in the same plane (Fig. 6*a*). The N···I distance is 2.995 (2) Å, corresponding to a 16% reduction in the sum of the van der Waals radii of I and N (Bondi, 1964) and the C—I···N angle is approximately 170.2 (1)°. The adopted *cis*-form makes the nitrogen lone pair more accessible to interact with the Lewis-acidic I atom, transforming the azo unit into a fairly good halogen-bond acceptor (Fig. 6*a*). This contact is quite short and comparable to the similar ones reported in the literature, for instance in the complex between in diazobicyclooctane and CBr_4 (Blackstock & Kochi, 1987) or in a metal–organic coordination polymer (Fernandez-Palacio, Saccone *et al.*, 2016). The strength of the observed halogen bonding has been estimated by theoretical calculations at the density functional theory level to be around 18.34 kJ mol^{-1}. The effectiveness of the I atom as a halogen-bond donor is further highlighted by the molecular electrostatic potential of **CIS**$_{azo}$ (Fig. 6*b*), where the positive σ-hole on the I atom located on the extension of the C—I bond (Politzer *et al.*, 2007), and the negative area associated with the lone pairs of the azo group, are clearly evident.

Similar to the **TRANS**$_{azo}$ derivative, in the packing of **CIS**$_{azo}$ a strong tendency of the aliphatic chains towards phase segregation is observed (Fig. 7*a*). Conversely, no arene–perfluoroarene quadrupolar interactions are detected (Fig. 7*b*). These observations highlight that the halogen-bonding contacts and the segregation of the alkyl chains cooperatively stabilize the molecular packing of the **CIS**$_{azo}$ molecule.

Defining the two planes containing either aromatic rings, a tilt angle of 61.66 (12)° is observed between them. Due to the tilting of the rings, one of the *ortho*-substituents in both rings is located quite close to the *ipso*-carbon of the adjacent ring. The distance between one of the *ortho*-fluorines and the *ipso*-carbon is 2.839 (4) Å, which is less than the sum of their van der Waals radii (3.17 Å). The same holds for the distance between one of the *ortho*-H atoms and the *ipso*-carbon (2.501 Å; the sum of the vdW radii is 2.90 Å). In fact, the QTAIM analysis (Bader, 1991) shows two unusual bond critical points, indicating a bonding interaction between the *ortho*-substituents and the *ipso*-C atoms (Fig. 8). Interacting quantum atom (IQA; Blanco *et al.*, 2005; Francisco *et al.*, 2006) analysis was performed to further study these bonding interactions.

The most relevant values of the QTAIM and IQA analyses are presented in Table 2. The small, positive values for the electron densities (ρ) and the Laplacians of the electron densities ($\nabla^2\rho$) at the aforementioned bond critical points indicate that the interactions are of weak, closed-shell type. The negative interaction energies (E_{inter}) suggest that the interactions are stabilizing, and that the C···F interaction is

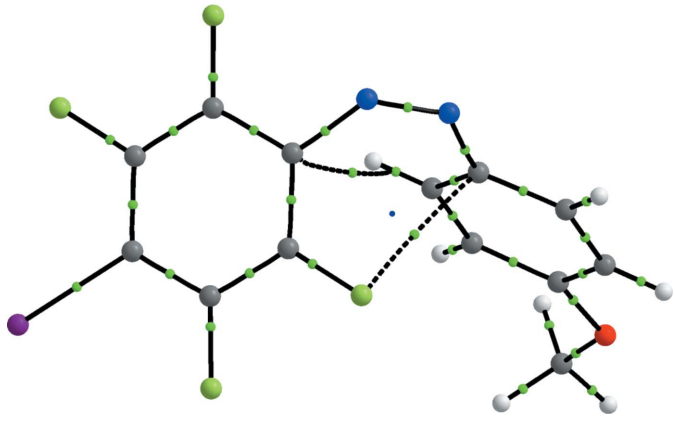

Figure 8
QTAIM analysis of the **CIS**$_{azo}$ molecule. Bond critical points are shown as green dots.

significantly stronger than the C···H interaction. The interaction energies have been further divided into electrostatic (E_{cl}) and exchange (E_x) components. A comparison of the components show that the stabilizing energy of the C···F interaction is mainly due to the classical electrostatic, or Coulombic, energy component with only a small contribution from the exchange energy component. The energy of the much weaker C···H interaction, however, is mainly due to the exchange energy component. Even if further studies are needed to support this claim, we believe that such stabilizing C···F interactions play an important role in dictating the unprecedented stability of the *cis*-forms of fluorinated azobenzenes (Bléger *et al.*, 2012; Knie *et al.*, 2014).

4. Conclusions

We have reported the crystal structures of *trans*- and *cis*-isomers of a fluorinated azobenzene shown in Fig. 1. The analysis of their structures in the solid state revealed an arrangement of the molecules that is profoundly different for the two isomers. In the *cis*-isomer structure, halogen bonding between neighboring molecules provides a stabilizing contribution to the overall packing, while in the *trans*-isomer, a major contribution is given by arene–perfluoroarene quadrupolar interactions. Our investigation is a step towards more comprehensive understanding of the role of non-covalent interactions in driving the crystal packing of metastable isomers of photoresponsive molecules, paving the way towards devising photomobile crystals of fluorinated azobenzenes bearing long alkyl chains.

Acknowledgements

AP gratefully acknowledges the Academy of Finland Research Fellowship program (Decision Nos. 277091 and 284553), and the Emil Aaltonen Foundation for financial support. AS is thankful to Professor Ángel Martín Pendás for helpful discussions regarding the Interacting Quantum Atoms analysis.

References

Bader, R. F. W. (1991). *Chem. Rev.* **91**, 893–928.
Bandara, H. M. D. & Burdette, S. C. (2012). *Chem. Soc. Rev.* **41**, 1809–1825.
Beharry, A. A., Sadovski, O. & Woolley, A. G. (2011). *J. Am. Chem. Soc.* **133**, 19684–19687.
Blackstock, S. C. & Kochi, J. K. (1987). *J. Am. Chem. Soc.* **109**, 2484–2496.
Blanco, M. A., Martín Pendás, A. & Francisco, E. (2005). *J. Chem. Theory Comput.* **1**, 1096–1109.
Bléger, D. & Hecht, S. (2015). *Angew. Chem. Int. Ed.* **54**, 11338–11349.
Bléger, D., Schwarz, J., Brouwer, A. M. S. & Hecht, S. (2012). *J. Am. Chem. Soc.* **134**, 20597–20600.
Bondi, A. (1964). *J. Phys. Chem.* **68**, 441–451.
Boys, S. F. & Bernardi, F. (1970). *Mol. Phys.* **19**, 553–566.
Bruker (2008). *APEX2, SAINT* and *SADABS.* Bruker AXS Inc. Madison, Wisconsin, USA.
Burla, M. C., Camalli, M., Carrozzini, B., Cascarano, G. L., Giacovazzo, C., Polidori, G. & Spagna, R. (2003). *J. Appl. Cryst.* **36**, 1103.
Bushuyev, O. S., Corkery, T. C., Barrett, C. J. & Friščić, T. (2014). *Chem. Sci.* **5**, 3158–3164.
Bushuyev, O. S., Tan, D., Barrett, C. J. & Friščić, T. (2015). *CrystEngComm*, **17**, 73–80.
Bushuyev, O. S., Tomberg, A., Friščić, T. & Barrett, C. J. (2013). *J. Am. Chem. Soc.* **135**, 12556–12559.
Cavallo, G., Metrangolo, P., Milani, R., Pilati, T., Priimagi, A., Resnati, G. & Terraneo, G. (2016). *Chem. Rev.* **116**, 2478–2601.
Corradi, E., Meille, S. V., Messina, M. T., Metrangolo, P. & Resnati, G. (2000). *Angew. Chem. Int. Ed.* **39**, 1782–1786.
Fernandez-Palacio, F., Poutanen, M., Saccone, M., Siiskonen, A., Terraneo, G., Resnati, G., Ikkala, O., Metrangolo, P. & Priimagi, A. (2016). *Chem. Mater.* **28**, 8314–8321.
Fernandez-Palacio, F., Saccone, M., Priimagi, A., Terraneo, G., Pilati, T., Metrangolo, P. & Resnati, G. (2016). *CrystEngComm*, **18**, 2251–2257.
Francisco, E., Martín Pendás, A. & Blanco, M. A. (2006). *J. Chem. Theory Comput.* **2**, 90–102.
Frisch, M. J. *et al.* (2009). *GAUSSIAN*09, Revision D.01. Gaussian, Inc., Wallingford, CT, USA.
Groom, C. R., Bruno, I. J., Lightfoot, M. P. & Ward, S. C. (2016). *Acta Cryst.* B**72**, 171–179.
Hoffmann, R. (1987). *Am. Sci.* **75**, 619–621.
Hoffmann, R., Schleyer, P. W. R. & Schaefer, H. III (2008). *Angew. Chem. Int. Ed.* **47**, 7164–7167.
Iamsaard, S., Anger, E., Aßhoff, S. J., Depauw, A., Fletcher, S. P. & Katsonis, N. (2016). *Angew. Chem. Int. Ed.* **55**, 9908–9912.
Keith, T. A. (2016). *TK Gristmill Software.* Overland Park KS, USA, http://aim.tkgristmill.com.
Kishikawa, K. (2012). *Isr. J. Chem.* **52**, 800–808.
Knie, C., Utecht, M., Zhao, F., Kulla, H., Kovalenko, S., Brouwer, A. M., Saalfrank, P., Hecht, S. & Bléger, D. (2014). *Chem. Eur. J.* **20**, 16492–16501.
Macrae, C. F., Bruno, I. J., Chisholm, J. A., Edgington, P. R., McCabe, P., Pidcock, E., Rodriguez-Monge, L., Taylor, R., van de Streek, J. & Wood, P. A. (2008). *J. Appl. Cryst.* **41**, 466–470.
Politzer, P., Lane, P., Concha, M. C., Ma, Y. & Murray, J. S. (2007). *J. Mol. Model.* **13**, 305–311.
Priimagi, A., Cavallo, G., Forni, A., Gorynsztejn-Leben, M., Kaivola, M., Metrangolo, P., Milani, R., Shishido, A., Pilati, T., Resnati, G. & Terraneo, G. (2012). *Adv. Funct. Mater.* **22**, 2572–2579.
Priimagi, A., Saccone, M., Cavallo, G., Shishido, A., Pilati, T., Metrangolo, P. & Resnati, G. (2012). *Adv. Mater.* **24**, OP345–OP352.
Řezáč, J., Riley, K. E. & Hobza, P. (2012). *J. Chem. Theory Comput.* **8**, 4285–4292.
Saccone, M., Cavallo, G., Metrangolo, P., Pace, A., Pibiri, A., Pilati, T., Resnati, G. & Terraneo, G. (2013). *CrystEngComm*, **15**, 3102–3105.
Saccone, M., Cavallo, G., Metrangolo, P., Resnati, G. & Priimagi, A. (2015). *Top. Curr. Chem.* **359**, 147–166.
Salonen, L. M., Ellermann, M. & Diederich, F. (2011). *Angew. Chem. Int. Ed.* **50**, 4808–4842.
Samanta, S., Qin, C., Lough, A. J. & Woolley, A. (2012). *Angew. Chem. Int. Ed.* **51**, 6452–6455.
Sheldrick, G. M. (2008). *Acta Cryst.* A**64**, 112–122.
Siewertsen, R., Neumann, H., Buchheim-Stehn, B., Herges, R., Näther, C., Renth, F. & Temps, F. (2009). *J. Am. Chem. Soc.* **131**, 15594–15595.

Siiskonen, A. & Priimagi, A. (2017). *J. Mol. Model.* **23**, 50.
Tschierske, C. (2012). *Top. Curr. Chem.* **318**, 1–108.
Weston, C. E., Richardson, R. D., Haycock, P. R., White, A. J. P. & Fuchter, M. J. (2014). *J. Am. Chem. Soc.* **136**, 11878–11881.
Williams, J. H., Cockcroft, J. K. & Fitch, A. N. (1992). *Angew. Chem. Int. Ed.* **31**, 1655–1657.
Zhao, Y. & Ikeda, T. (2009). *Smart Light-Responsive Materials: Azobenzene-Containing Polymers and Liquid Crystals.* New York: Wiley.